Protective Effects of Gold Nanoparticles Against Malathion-Induced Cytotoxicity in Caco-2 Cells

Zeynab Shahmahmoodi[1], Somayeh Jafarinejad[2], Mohammad Reza Hormozi-Nezhad[3], Homanaz Ghafari[1], Mahmoud Ghazi-Khansari[1]

[1] Department of Pharmacology, School of Medicine, Tehran University of Medical Sciences, Tehran, Iran

[2] Finetech in Medicine Research Center, Iran University of Medical Sciences, Tehran, Iran

[3] Department of Chemistry, Sharif University of Technology, Tehran, Iran

Received: 08 Jun. 2020; Accepted: 19 Oct. 2020

Abstract- Malathion is an organophosphorus insecticide widely used in agriculture, residential area, and public health programs with a known mechanism of toxicity of inhibition of acetylcholinesterase and induction of oxidative stress. Gold nanoparticles (AuNPs) represent stable and easily synthesized nanoparticles with extensive use in consumer products and medicine. Due to the antioxidant property of AuNPs, it is possible that AuNPs may prevent malathion-induced oxidative damage. In this study, the cytotoxicity of malathion and AuNPs (10 and 20 nm) were measured separately in Caco-2 cells. Then the protective effects of AuNPs were evaluated by measuring the oxidative stress (lipid peroxidation level and glutathione content) and acetylcholinesterase activity. The calculated IC50s values at 48 hr were 326.8±0.32, 43.09±0.65, and 41.46±0.24 µg/ml for malathion, AuNPs 10 and 20 nm, respectively. Then, the lowest concentration of AuNPs (1 µg/ml) and IC50 concentration of malathion (326.8 µg/ml) were selected to evaluate the effects of pretreatment of Caco-2 cells with AuNPs before exposure to malathion were evaluated. Interestingly, the results showed remarkably significant protective effects of AuNPs by attenuation the different parameters of oxidative stress and cytotoxicity induced by malathion in cells (P<0.001). It is the first report showing the protective effects of AuNPs against malathion-induced cytotoxicity in the Caco-2 cell line.

Acta Med Iran 2020;58(11):552-561.

Keywords: Gold nanoparticles; Oxidative stress; Acetylcholinesterase; Malathion; Caco-2 cells; Cytotoxicity

Introduction

Nanotechnology is one of the rapidly growing fields in science and technology which deals with producing and applying materials at nanoscale dimensions (1). Nanomaterials have attracted much attention in various fields due to their unique physicochemical properties as the result of their nano-size and large surface area to volume ratio, which is the base of all various novel applications (2). Nanoparticles (NPs) are in a similar range size of most biological macromolecules make them appropriate in various biomedical applications, and their possible interaction with biological systems such as tissues and cells (3). Among the metallic NPs, gold nanoparticles (AuNPs) represent one of the stable, biocompatible, easily synthesized, size-tunable surface plasmon resonance, and easy-surface functionalized NPs which have been applied widely in imaging diagnosis (4), drug delivery (5), radiosensitization (6), and photothermal therapy (7).

Malathion (O, O-dimethyl-S-(1,2-dicarbethoxyethyl) phosphorodithioate) is an organophosphorus (OP) insecticide widely used in agriculture, residential area, public health programs against mosquito-borne illness, and also used in some lice shampoos (8). Due to the different applications of malathion, it can be present in the soil, air, surface water and groundwater, and food, in addition to occupational exposures. Malathion's low mammalian toxicity has turned it to be the most used organophosphate worldwide, so it is one of the main sources of occupational exposure to pesticides in residential, agricultural, and industrial settings. It has been reported that about 19,170 workers in the US, working in 18 occupations apart from farm and greenhouse labor, were potentially exposed to malathion in occupational settings (9). The level of occupational

Corresponding Author: M. Ghazi-Khansari
Department of Pharmacology, School of Medicine, Tehran University of Medical Sciences, Tehran, Iran
Tel: +98 2166402569 Fax: +98 2166402569, E-mail address: ghazikha@tums.ac.ir

exposure to malathion is varied according to factors such as task, application method, use of personal protective equipment, and personal hygiene (10).

Malathion is low toxic to human as a neurotoxic agent by irreversible inhibition of two mammalian cholinesterases (ChE), acetylcholinesterase (AChE) and butyrylcholinesterase. AChE is one of the critical enzymes in the synaptic space of the mammalian nervous system by catalyzing the breakdown of the neurotransmitter acetylcholine (ACh) into choline and acetic acid, which allows the nerve impulses transmission to cholinergic synapses. Inhibition of AChE causes the accumulation of ACh in the synaptic cleft resulting in disrupted neurotransmission (11,12). Although the inhibition of AChE has been recognized as the main mechanism of malathion toxicity, oxidative stress has also been reported as a possible mechanism in malathion-induced organ injury in mammals (13-15). The lipid peroxidation, protein oxidation, GSH depletion, and DNA single-strand breaks are all the consequences of oxidative stress damage of malathion cellular dysfunction and injury. The carcinogenicity, mutagenicity, and teratogenicity of malathion have also been studied a lot (10,16-18).

The “safe” and “nontoxic” assumption of AuNPs as a result of the inert characteristics of bulk gold caused their increased applications not only in biomedical fields but also in daily use goods such as cosmetics, toothpaste, and food supplements (19). Some reports indicated the cytotoxic effects of AuNPs on different cell lines, which depend on various parameters such as the size and concentrations of them (20). But on the other hand, a large number of studies confirmed AuNPs not only as a “nontoxic” material but also as a treatment in chronic inflammatory and autoimmune diseases (21-25). Also, the protective effects of AuNPs against oxidative stress-induced conditions such as hyperglycemia and osteoporosis by inhibition or elimination of ROS formation have been reported (26,27).

Considering oxidative stress induction as one of the cytotoxic mechanism of malathion and the proven antioxidant activity of AuNPs in several reports, it is of interest to investigate whether co-administration of AuNPs could protect the malathion-induced cytotoxicity. So, in this study, we first evaluated the cytotoxic effect of both malathion and citrate stabilized AuNPs (10 and 20 nm) on Caco-2 cells by MTT assay to find out the IC50 values. Then, the effects of the pretreatment of AuNPs on malathion treated cells have been evaluated by measuring the oxidative stress parameters (Lipid peroxidation and glutathione level). Caco-2 cells represent an ideal in vitro model for intestinal cells and widely used to assess the adsorption of orally administrated drugs, toxicants, and NPs (28). Caco-2 cell line has been used in systematic studies to evaluate the effects of NPs characteristics on various cellular responses (29-31).

Materials and Methods

Synthesis and characterization of gold nanoparticles (AuNPs)

AuNPs were synthesized by the modification of the traditional Frens method in two different sizes of 10 and 20 nm. In this method, monodisperse citrate-stabilized AuNPs were obtained with seed-mediated strategy by the reduction of HAuCl4 with sodium citrate (32). Briefly, gold seeds (~10 nm AuNPs) were prepared by injecting an aqueous HAuCl4 precursor solution into a boiling solution of sodium citrate, and the reaction was run until it reached a red-wine color. Then, the temperature of the mentioned solution was decreased to 90° C, and more sodium citrate and HAuCl4 precursor were injected as a growth step in order to synthesize 20 nm AuNPs. Three of such growth steps were needed to increase the particle size from ~10 to ~20 nm. Transmission electron microscopy (TEM) analysis was carried out by TEM EM 900 ZEISS. Particle size distributions were determined through dynamic light scattering (Malvern Instruments, model Zetasizer Nano ZS 3600). The Nano ZS instrument was also used to measure the zeta potential.

Cell culture

The Caco-2 cell line was obtained from the Iranian Biological Resource Center (IBRC). The cells were grown in DMEM/F-12 culture medium (Biosera, France) supplemented with 10% (v/v) heat-inactivated fetal bovine serum (Gibco, American) and 1% (v/v) penicillin-streptomycin antibiotics (Biowest, France) at 37° C and 5% (v/v) CO2 in a humidified incubator.

Cytotoxicity evaluation by MTT assay

The cytotoxicity of AuNPs and malathion in Caco-2 cells was determined by MTT assay (33). Cells were seeded in a 96-well plate at the density of 3×104 cells. After overnight culture, cells were treated with 100 µL of different concentrations of malathion (165-1000 µg/ml) and AuNPs 10 and 20 nm (1-55 µg/ml) separately. After the 48 h incubation, 20 µL of MTT solution was added to each well and incubated for 3-4 h. Then the plates were reversed, and 100 µL of DMSO was added to each well, and the absorbance was measured at 570 nm by ELISA reader (Synergy HT, Biotek). The data of MTT assay was

used to calculate the IC50 values of malathion and AuNPs, and also to select the suitable concentrations of them for the rest of the experiments .

Measurements of oxidative stress

Lipid peroxidation measurement

The amount of cellular lipid peroxidation was measured by a colorimetric method according to the malondialdehyde (MDA) assay kit instruction (ZellBio GmbH-Germany). Caco-2 cells were seeded in a 6-well plate at the density of 3×105 cells for 24 h and then treated with the selected concentrations of malathion and AuNPs 10 and 20 nm for 48 h. At the end of exposure time, cells were trypsinized and washed with PBS. Cells were centrifuged at 2000-3000 rpm for 5 minutes, lysed in HIS buffer, and freeze-thawed twice. MDA is measured in an acidic media at 535 nm colorimetrically (34).

Determination of glutathione (GSH) level

The total amount of the cellular GSH content was measured by a colorimetric method according to the Glutathione assay kit instruction (ZellBio GmbH-Germany). Caco-2 cells were seeded in a 6-well plate at the density of 3×105 cells for 24 h and then treated with the selected concentrations of malathion and AuNPs 10 and 20 nm for 48 h. At the end of the exposure time, cells were trypsinized and washed with PBS. Cells were centrifuged at 2000-3000 rpm for 5 minutes, lysed in HIS buffer, and freeze-thawed twice. The measurement of GSH was done by a kinetic assay in which the catalytic amounts of GSH causes a continuous reduction of 5,5-dithiobis (2-nitrobenzoic acid) to 5-thio-2-nitrobenzoic acid (TNB). The formed oxidized glutathione GSSG is recycled by glutathione reductase and NADPH. The yellow product of TNB was measured by an ELISA reader at 412 nm (35).

Measurements of AChE activity (Ellman assay)

Extraction of AChE

We used the Ellman assays protocol to extract and measure AChE activity (36). Cells were harvested by trypsinization and washed three times with PBS. For extracting the cells, 0.5 ml of high ionic strength (HIS) buffer (10 mM NaHPO4 pH 7.0-8.0, 1 M NaCl, 10% Triton X-100, 1 mM EDTA) was added to each well and incubated 5-10 minutes at the room temperature. Then the cell suspension was centrifuged at 12,000 rpm in a 15 ml Cortex tube for 20 minutes. The supernatant was transferred to an appropriate storage tube and stored at -80◦ C for the enzyme activity and protein assay measurements.

Measurement of AChE Activity

To measure the enzyme activity of AChE, 72.5 µL potassium phosphate buffer (75 mm L-1, pH 7.9), 2 µL substrate (Acetylthiocholine iodide 3 mm L-1), and 5 µL Ellman reagent (DTNB, 5,5'-Dithio-bis-nitrobenzoic acid, 0.25 mm L-1) were mixed in each well of 96-well plate and then 72.5 µL of cell lysate supernatant was added to wells, and the absorbance was read at 405 nm by ELISA reader immediately .

Protein measurement

The Bradford protein assay protocol was used to measure cell protein concentration (37). A serial dilution of the known range of concentrations of bovine serum albumin (BSA) (Sigma-Aldrich) was prepared, and then the unknown protein samples (cell lysate supernatants) were diluted to be within the range of the assay. 5 µL of dilutions was added to the wells of a 96-well plate, and 250 µL of Bradford reagent was added to each well and mixed well. After 5 min incubating at room temperature, the absorbance was measured at 595 nm. The protein concentrations of unknown samples were obtained via the standard curve .

Calculation of AChE activity

After measuring the AChE absorbance and protein concentrations of cells, we convert out data into the standardized units of micromoles substrate hydrolyzed per minute per ml of plasma using the extinction coefficient for the yellow product (13,600 M-1 cm-1). AChE activity was calculated by using the following formula (36).

AChE activity (µmol/min) = $\Delta A/\Delta t \times Vt/Vs. \times 1/C$ where

$\Delta A/\Delta t$ (Rate) = the line gradient of the absorption curve

Vt = Total volume (µL(

Vs = Sample volume (µL(

C = Cells protein concentration (mg/mL(

Statistics

All experiments were done in triplicates repeated in three independent experiments, and the data were presented as the mean±standard deviation (SD). IC50 values were calculated by using a four-parameter logistic equation. Data were plotted as an inhibition dose-response curve with variable slope using GraphPad Prism software (version 6.01). Multiple comparisons and comparisons versus the control were performed with one-way ANOVA. Differences were considered significant at $P<0.05$.

Results

Characterization of gold nanoparticles

AuNPs were synthesized by a seed-mediated method using HAuCl4, a precursor salt. Physical characteristics of the nanoparticles were confirmed using TEM, as shown in Figure 1 A1 and B1. The range of observed diameters of the synthesized gold nanoparticles was about 12 and 20 nm, relatively uniform in diameter and spherical in shape. Due to the importance of size distribution and zeta potential of nanoparticles in bio-interactions, these parameters were also measured (Figure 1 A2-3 and B2-3). The results showed that the DLS and zeta potential of 10 nm AuNPs were 10±2.27 nm, monodispersed (PDI: 0.23) with the zeta potential of -4.76 mV. For 20 nm AuNPs, the average size was 19.5±7.72 nm, monodispersed (PDI: 0.29) with a zeta potential of -28.1 mV.

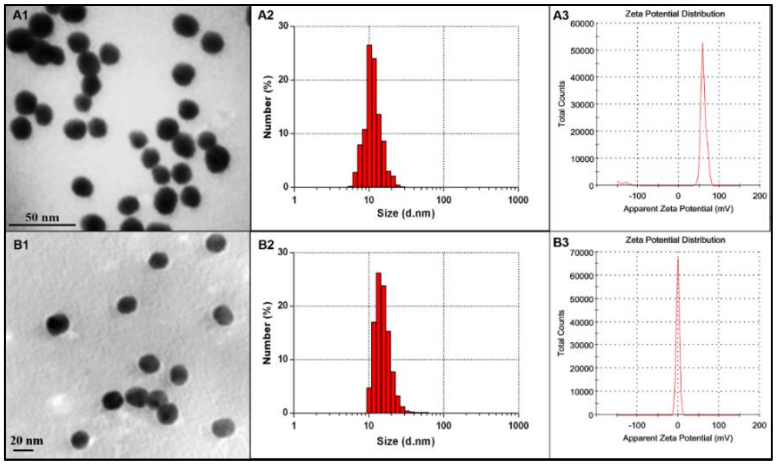

Figure 1. Characterization of AuNPs 10 (A) and 20 nm (B). (1) TEM images (2) DLS measurements and (3) Zeta potential

The cytotoxicity of malathion and AuNPs in Caco-2 cells by MTT

The MTT assays were performed to investigate the cytotoxic effects of malathion and AuNPs in the Caco-2 cell line. The cytotoxicity of malathion on Caco-2 cells was found to be concentration-dependent, with an IC50 value of 326.8±0.32 µg/ml at 48 h (Figure 2).

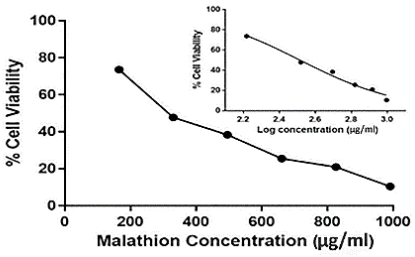

Figure 2. The viability of Caco-2 cells treated with different concentrations of malathion at 48 h. Data are presented as the mean ± SD from three independent experiments of three replicates. The inset shows the graph of the cell viability versus the log of malathion concentrations with its nonlinear curve fitting

The results demonstrated a slight decrease in IC50 values of malathion from time 24 h to 72 h, which shows the time-dependent of malathion cytotoxicity (Table 1). Based on the MTT result, the IC50 value of malathion at 48 h was selected as the desired concentration for further experiments in order to be sure to observe the cytotoxicity of malathion.

The IC50 values of AuNPs at 48 h were 43.09 and 41.46 µg/ml for 10 and 20 nm, respectively. The cytotoxicity of AuNPs was size and dose-dependent (Figure 3). Furthermore, the results showed that the IC50 value slightly increased from 24 h to 72 h, showing that the cytotoxic effects decreased over time (Table 1). We selected a concentration of 1 µg/ml of AuNPs with no cytotoxicity effect for further experiments.

The protective effects of AuNPs against malathion-induced cytotoxicity in Caco-2 cells

The MTT assay was performed to evaluate the cytotoxic effects of malathion in the presence of AuNPs. To do this, the Caco-2 cells were pretreated with 1 µg/ml of AuNPs for a half-hour, and then 326.8 µg/ml of malathion was added to the cells. In order to see the cytotoxic effect of the ionic form of gold, HAuCl4 (1 µg/ml) also was used as control. Results showed that the viability of cells pretreated with AuNPs was significantly improved compared to the malathion group (P<0.001) (Figure 4). Also, the smaller size of AuNPs (10 nm)

showed a more protective effect compared to 20 nm (P<0.001).

Table 1. The IC50 values of malathion and AuNPs (10 and 20 nm) in Caco-2 cells were measured by the MTT assay. Data expressed as Mean ± SD, n =3 of three replicates.

Time (h)	Malathion (µg/ml)	AuNPs (µg/ml)	
		10 nm	20 nm
24	328.5±0.76	42.48±0.55	41.08±0.66
48	326.8±0.32	43.09±0.65	41.46±0.24
72	323.7±0.58	44.18±0.25	42.98±0.32

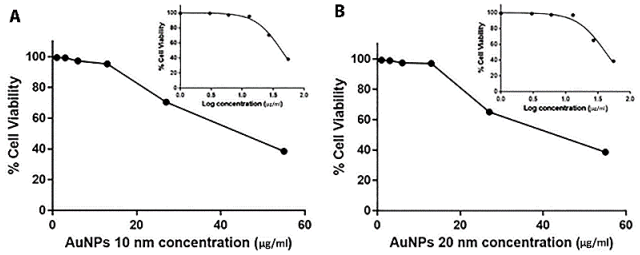

Figure 3. The viability of Caco-2 cells treated with different concentrations of AuNPs 10 (A) and 20 nm (B) at 48 h by the MTT assay. Data are presented as the mean ± SD from three independent experiments. The insets show the graph of the cell viability versus the log of AuNPs concentrations and their nonlinear curve fitting

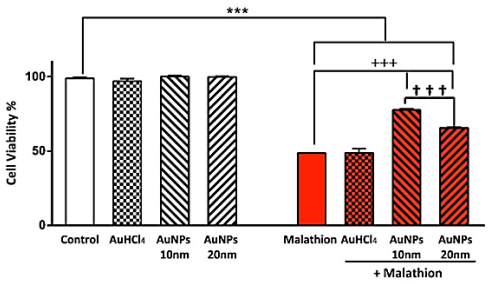

Figure 4. The cell viability of Caco-2 treated with HAuCl4, AuNPs 10 and 20 nm (1µg/ml), and malathion (326.8 µg/ml) at 48 h. The right side of the graph shows the viability of Caco-2 cells pretreated with 1 µg/ml of HAuCl4 or AuNPs and then exposed to malathion (326.8 µg/ml). Data were presented as the mean ± SD from three independent triplicate experiments. *** P<0.001 compared with the control group, +++ P<0.001 compared to malathion group and ††† P<0.001 compared to AuNPs 10 nm

Evaluation of the antioxidant effect of AuNPs against malathion-treated Caco-2 cells

Lipid peroxidation measurement

The MDA assay was performed to measure the lipid peroxidation level of Caco-2 cells exposed to AuNPs, Au salt (HAuCl4), and malathion. Also, the lipid peroxidation level of cells pretreated with 1 µg/ml of AuNPs and HAuCl4 on exposed cells to malathion were measured separately. The results showed no significant differences in MDA amount between AuNPs and the Au salt compared to the control group (Figure 5). The MDA levels were higher in all malathion-treated cells compared to the control group (P<0.001). The pretreatment of cells with AuNPs (not the ionic form) could decrease the MDA level compared to malathion treated cells, which showed the protective effect of AuNPs against lipid peroxidation (P<0.001). Also, the smaller size of AuNPs (10 nm) has a better improvement effect on the MDA level compared to the 20 nm size (P<0.05).

GSH measurements

The GSH assay was performed to determine the GSH level of Caco-2 exposed to 1 µg/ml of AuNPs (10 and 20 nm), $HAuCl_4$, and malathion (326.8 µg/ml). Also, the GSH level of pretreated cells with AuNPs and $HAuCl_4$ on exposed cells to malathion was determined separately. The results showed no significant differences in GSH amount between AuNPs and the Au salt compared to the control group (Figure 6). The malathion treatment depleted GSH in all treated groups (P<0.001). A weaker depletion of GSH was observed in pretreated cells with AuNPs (not ionic form) compared to malathion

(*P*<0.001). The smaller size of AuNPs (10 nm) showed more improvement compared to the 20 nm size (*P*<0.01).

Evaluation of the anti-cholinesterase activity of AuNPs against malathion-treated Caco-2 cells

AChE activity of Caco-2 cells exposed to 1 µg/ml of AuNPs, and Au salt ($HAuCl_4$), malathion (326.8 µg/ml) was shown in Figure 7. Also, the effects of pretreatment of the cells with 1 µg/ml of AuNPs and $HAuCl_4$ on exposed cells to malathion were investigated separately. The results showed that AuNPs and the ionic form of Au had no effect on AChE activity. Malathion inhibited the AChE activity significantly (*P*<0.001). Pretreatment of cells with AuNPs (not the ionic form) could significantly improve the inhibitory effect of malathion (*P*<0.001). Also, the smaller size of AuNPs (10 nm) has a better improvement effect compared to the bigger size (*P*<0.001).

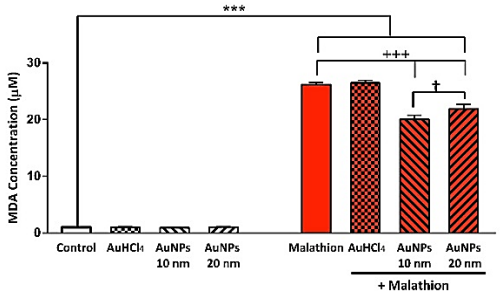

Figure 5. The MDA levels of Caco-2 cells were treated with 1 µg/ml of HAuCl4, AuNPs 10 and 20 nm, and 326.8 µg/ml malathion at 48 h. The right side of the graph shows the MDA level of cells pretreated with 1 µg/ml of HAuCl4, AuNPs 10 and 20 nm and then exposed to malathion. Data are presented as the mean ± SD from three independent triplicate experiments. *** *P*<0.001 compared with control group, +++ *P*<0.001 compared to malathion group and † *P*<0.05 compared to AuNPs 10 nm

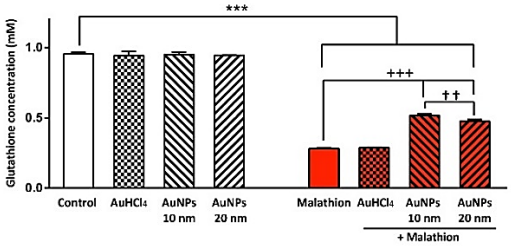

Figure 6. The GSH level of Caco-2 cells treated with 1 µg/ml of HAuCl4, AuNPs 10 and 20 nm, and 326.8 µg/ml malathion at 48 h. The right side of the graph shows the glutathione level of cells pretreated with 1 µg/ml of HAuCl4, AuNPs 10 and 20 nm and then exposed to malathion. Data are presented as the mean±SD from three independent triplicate experiments. *** *P*<0.001 compared with control group, +++ *P*<0.001 compared to malathion group and†† *P*<0.01 compared to AuNPs 10 nm

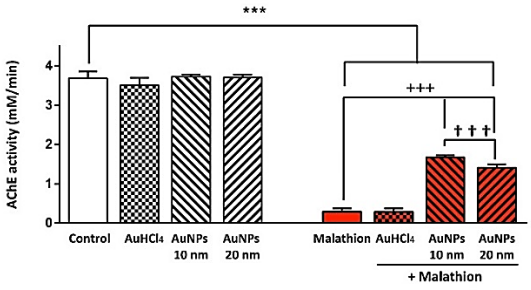

Figure 7. The activity of AChE in Caco-2 cells treated with 1 µg/ml of HAuCl4, AuNPs 10 and 20 nm, and 326.8 µg/ml malathion at 48 h. The right side of the graph shows the AChE activity of cells pretreated with 1 µg/ml of HAuCl4, AuNPs 10 and 20 nm and then exposed to malathion. Data are presented as the mean ± SD from three independent triplicate experiments. *** *P*<0.001 compared with the control group, +++ *P*<0.001 compared to malathion group and ††† *P*<0.001 compared to AuNPs 10 nm

Discussion

In the present study, the cytotoxicity, oxidative stress, and AChE activity of malathion and AuNPs, and the impact of AuNPs presence in cell growth media on malathion-induced cytotoxicity were investigated in Caco-2 cells .

All the results showed the cytotoxic effects of malathion on Caco-2 cells with a strong concentration-dependent relationship with IC50 328.5±0.76 µg/ml at 48h exposure time. The cytotoxicity of malathion was confirmed by inhibition of AChE activity, increased level of LPO, and the depletion level of GSH. Previous in-vitro studies reported the cytotoxic effects of malathion on different cell lines such as human lymphoid cells (38), murine T-lymphocyte (CTL) model (39), grass carp cell line (40), human erythrocytes (13), and HepG2 cells (15). The cellular effects of malathion and the mechanisms involved have been clearly discussed in these reports. Our results were in good agreement with them regarding the concentration and time dependency of malathion cytotoxicity on the Caco-2 cell (Table 1). Previous studies explained the mechanism of malathion-induced cellular oxidative stress, such as lipid peroxidation and glutathione depletion (13,41). The elevated level of MDA has been shown as a marker of malathion cytotoxicity on cells (13,15). The detoxification of OPs by conjugation with cellular GSH leads to depletion of GSH content as the indication of the significant occurrence of cellular oxidative stress (42). Our results showed that treating Caco-2 cells with malathion significantly increased the MDA level (P<0.001) and depleted the GSH level up to 70% compared to the control group (P<0.001). Inhibition of AChE activity is the most important toxic effect of OP compounds on living organisms, which has been demonstrated in some in-vivo and in-vitro studies (43,44). Our results showed that the IC50 concentration of malathion could inhibit the AChE by 95% in the Caco-2 cell line (P<0.001), which was consistent with previous results on different cell lines.

Regarding AuNPs, our results showed no cytotoxic effects at low concentrations of nanoparticles. By increasing the concentration, the viability of Caco-2 cells was decreased in a dose-response manner exhibiting the typical sigmoidal curve with calculated IC50s 43.09±0.65 and 41.46±0.24 µg/ml at 48 h for AuNPs 10 and 20 nm, respectively. A previous study on Caco-2 cells showed that only exposure to a small size of AuNPs (5 nm) at relatively high concentrations could inhibit the cell growth and decrease colony-forming efficiency (30). Absorption, accumulation, and cytotoxicity of different sizes of AuNPs (15, 50, 100 nm) on Caco-2 cells have been evaluated previously and revealed the relationship between the evaluated parameters and the particle size of AuNPs (29). Several other studies have shown that the cytotoxicity of AuNPs is dependent on their cellular uptake, which in turn is related to the size, shape, concentration, aggregation state, surface coating, and surface charge of NPs (21,31,45,46).

In this study, we evaluated the effect of AuNPs on the cytotoxicity of malathion on the Caco-2 cell line. Pretreatment of cells with AuNPs, even at low concentration (1 µg/ml), significantly attenuated the malathion-induced cytotoxicity by increasing the cell viability, AChE activity, GSH content, and decreasing LPO level. These results indicated that AuNPs might have a beneficial and protective effect against malathion-induced cytotoxicity. This is the first study that showed the protective effect of AuNPs against OP-induced cytotoxicity. Previously it was published that spherical AuNPs could detect and removed OP insecticides such as malathion and dimethoate from aqueous solution and water contaminants by adsorption with high efficiency (47,48). This property of AuNPs has been used to develop a rapid colorimetric assay for visual detection of OP insecticides based on the clear color shift during the aggregation of AuNPs induced by analytes, which is AChE in this assay (49-52). Our result showed that pretreatment of cells with AuNPs before exposure to malathion significantly increased the cell viability and AChE activity compared to the malathion treated group (P<0.001). Due to the adsorption property of AuNPs, it may conclude that AuNPs in cell media culture could adsorb some malathion and, therefore, decrease the cytotoxic effect of malathion. The better protective effect of 10 nm size of AuNPs compared to 20 nm could be due to the higher surface area to volume ratio of the smaller size and so, a greater capacity to absorb more malathion .

We demonstrated that malathion induced oxidative stress in CaCo-2 cells through increasing of LPO and depletion of GSH content (Figure 5 and 6). But, pretreatment of cells with AuNPs significantly neutralized the extent of oxidative stress (P<0.001). One proposed mechanism of antioxidative activity of AuNPs could be through their oxygen scavenging property. Previous studies have indicated that AuNPs have strong activity in scavenging free radicals (53,54). Also, another study confirmed that AuNPs increased the enzymes

involved in the antioxidant defense, including GSH and SOD, and a decrease in lipid peroxidation (27). According to these studies and the results of our study, it can be suggested that AuNPs have the potential to exert cytoprotective effects against malathion-induced oxidative stress in Caco-2 cells.

In conclusion, AuNPs showed protective effects against malathion-induced cytotoxicity and oxidative stress, which was confirmed by increasing the cell viability, AChE activity, and recovered LPO and GSH levels in Caco-2 cells. The proposed mechanism could be due to the absorbency property of AuNPs for OP insecticides and/or the antioxidant property of AuNPs. Further researches are required in order to determine the exact mechanism of the protective effect of AuNPs in OP-induced cytotoxicity.

References

1. Dowling AP. Development of nanotechnologies. Mater Today 2004;7:30-5.
2. Rao CNR, Müller A, Cheetham AK. The chemistry of nanomaterials: synthesis, properties and applications. USA: John Wiley & Sons, 2006.
3. Sun H, Jia J, Jiang C, Gold S. Nanoparticle-Induced Cell Death and Potential Applications in Nanomedicine. International Int J Mol Sci 2018;19:754.
4. Boisselier E, Astruc D. Gold nanoparticles in nanomedicine: preparations, imaging, diagnostics, therapies and toxicity. Chem Soc Rev 2009;38:1759-82.
5. Ghosh P, Han G, De M, Kim CK, Rotello VM. Gold nanoparticles in delivery applications. Adv Drug Deliv Rev 2008;60:1307-15.
6. Chithrani DB, Jelveh S, Jalali F, Van Prooijen M, Allen C, Bristow RG, et al. Gold nanoparticles as radiation sensitizers in cancer therapy. Radiat Res 2010;173:719-28.
7. Huang X, Jain PL, El-Sayed IH, El-Sayed MA. Plasmonic photothermal therapy (PPTT) using gold nanoparticles. Lasers Med Sci 2008;23:217-28.
8. Idriss S, Levitt J. Malathion for head lice and scabies: treatment and safety considerations. J Drugs Dermatol 2009;8:715-20.
9. Wilson JD. Toxicological profile for malathion. Agency for Toxic Substances and Disease Registry, 2003.
10. IARC Working Group on the Evaluation of Carcinogenic Risks to Humans. Some organophosphate insecticides and herbicides, 2017.
11. Holmstedt B. Pharmacology of organophosphorus cholinesterase inhibitors. Pharmacol Rev 1959;11:567-688.
12. Mangas, I, Estevez J, Vilanova E, França TC. New insights on molecular interactions of organophosphorus pesticides with esterases. Toxicology 2017;376:30-43.
13. Durak D, Gökce Uzun F, Kalender S, Ogutcu A, Uzunhisarcikli M, Kalender Y. Malathion-induced oxidative stress in human erythrocytes and the protective effect of vitamins C and E in vitro. Environ Toxicol 2009;24:235-42.
14. John S, Kale M, Rathore N, Bhatnagar D. Protective effect of vitamin E in dimethoate and malathion induced oxidative stress in rat erythrocytes. J Nutr Biochem 2001;12:500-4.
15. Moore PD, Yedjou CG, Tchounwou PB. Malathion-induced oxidative stress, cytotoxicity, and genotoxicity in human liver carcinoma (HepG2) cells. Environ Toxicol 2010;25:221-6.
16. Bonner MR, Coble J, Blair A, Beane Freeman LE, Hoppin JA, Sandler DP, et al. Malathion exposure and the incidence of cancer in the agricultural health study. Am J Epidemiol 2007;166:1023-34.
17. Giri S, Prasad SB, Giri A, Sharma GD. Genotoxic effects of malathion: an organophosphorus insecticide, using three mammalian bioassays in vivo. Mutat Res 2002;514:223-31.
18. Khera K, Whalen C, Trivett G. Teratogenicity studies on linuron, malathion, and methoxychlor in rats. Toxicol Appl Pharmacol 1978;45:435-44.
19. Gioria S, Vicente JL, Barboro P, La Spina R, Tomasi G, Urbán P, et al. A combined proteomics and metabolomics approach to assess the effects of gold nanoparticles in vitro. Nanotoxicology 2016;10:736-48.
20. Chueh PJ, Liang RY, Lee YH, Zeng ZM, Chuang SM. Differential cytotoxic effects of gold nanoparticles in different mammalian cell lines. J Hazard Mater 2014;264:303-12.
21. Connor EE, Mwamuka J, Gole A, Murphy CJ, Wyatt MD. Gold nanoparticles are taken up by human cells but do not cause acute cytotoxicity. Small 2005;1:325-7.
22. Shukla R, Bansal V, Chaudhary M, Basu A, Bhonde RR, Sastry M. Biocompatibility of gold nanoparticles and their endocytotic fate inside the cellular compartment: a microscopic overview. Langmuir 2005;21:10644-54.
23. Mukherjee P, Bhattacharya R, Wang P, Wang L, Basu S,. Nagy JA, et al. Antiangiogenic properties of gold nanoparticles. Clin Cancer Res 2005;11:3530-4.
24. Rizwan H, Mohanta J, Si S, Pal A. Gold nanoparticles reduce high glucose-induced oxidative-nitrosative stress regulated inflammation and apoptosis via tuberin-mTOR/NF-κB pathways in macrophages. Int J Nanomedicine 2017;12:5841-62.
25. Chen, YS, Hung YC, Liau I, Huang GS. Assessment of the in vivo toxicity of gold nanoparticles. Nanoscale Res Lett

2009;4:858-64.
26. Suh KS, Lee YS, Seo SH, Kim YS, Choi EM. Gold nanoparticles attenuates antimycin A-induced mitochondrial dysfunction in MC3T3-E1 osteoblastic cells. Biol Trace Elem Res 2013;153:428-36.
27. BarathManiKanth S, Kalishwaralal K, Sriram M, Pandian SR, Youn HS Eom S, et al. Antioxidant effect of gold nanoparticles restrains hyperglycemic conditions in diabetic mice. J Nanobiotechnology 2010;8:16.
28. Hidalgo IJ, Raub TJ, Borchardt RT. Characterization of the human colon carcinoma cell line (Caco-2) as a model system for intestinal epithelial permeability. Gastroenterology 1989;96:736-49.
29. Yao M, He L, McClements DJ, Xiao H. Uptake of gold nanoparticles by intestinal epithelial cells: impact of particle size on their absorption, accumulation, and toxicity. J Agric Food Chem 2015;63:8044-9.
30. Bajak E, Fabbri M, Ponti J, Gioria S, Ojea-Jiménez I, Collotta A, et al., Changes in Caco-2 cells transcriptome profiles upon exposure to gold nanoparticles. Toxicol Lett 2015;233:187-199.
31. Aueviriyavit S, Phummiratch D, Maniratanachote R. Mechanistic study on the biological effects of silver and gold nanoparticles in Caco-2 cells–induction of the Nrf2/HO-1 pathway by high concentrations of silver nanoparticles. Toxicol Lett 2014;224:73-83.
32. Bastús NG, Comenge J, Puntes V. Kinetically controlled seeded growth synthesis of citrate-stabilized gold nanoparticles of up to 200 nm: size focusing versus Ostwald ripening. Langmuir 2011;27:11098-105.
33. Morgan DML. Tetrazolium (MTT) Assay for Cellular Viability and Activity. Methods Mol Biol 1998;79:179-83.
34. Armstrong D, Browne R. The Analysis of Free Radicals, Lipid Peroxides, Antioxidant Enzymes and Compounds Related to Oxidative Stress as Applied to the Clinical Chemistry Laboratory. In: Armstrong D, eds. Free Radicals in Diagnostic Medicine. Advances in Experimental Medicine and Biology. Boston, MA: Springer, 1994:43-58.
35. Rahman I, Kode A, Biswas SK. Assay for quantitative determination of glutathione and glutathione disulfide levels using enzymatic recycling method. Nat Protoc 2006;1:3159-65.
36. Ellman GL, Courtney KD, Andres V Jr, Feather-Stone RM. A new and rapid colorimetric determination of acetylcholinesterase activity. Biochem Pharmacol 1961;7:88-95.
37. Bradford MM. A rapid and sensitive method for the quantitation of microgram quantities of protein utilizing the principle of protein-dye binding. Anal Biochem 1976;72:248-54.
38. Sobti RC, Krishan A, Pfaffenberger CD. Cytokinetic and cytogenetic effects of some agricultural chemicals on human lymphoid cells in vitro: organophosphates. Mutat Res 1982;102:89-102.
39. Rodgers KE, Grayson MH, Imamura T, Devens BH. In vitro effects of malathion and O, O, S-trimethyl phosphorothioate on cytotoxic T-lymphocyte responses. Pestic Biochem Physiol 1985;24:260-6.
40. Chen Xy, Shao JZ, Xiang LX, Liu XM. Involvement of apoptosis in malathion-induced cytotoxicity in a grass carp (Ctenopharyngodon idellus) cell line. Comp Biochem Physiol C Toxicol Pharmacol 2006;142:36-45.
41. Malik J, Summer K. Toxicity and metabolism of malathion and its impurities in isolated rat hepatocytes: role of glutathione. Toxicol Appl Pharmacol 1982;66:69-76.
42. Karami-Mohajeri S, Abdollahi M. Toxic influence of organophosphate, carbamate, and organochlorine pesticides on cellular metabolism of lipids, proteins, and carbohydrates: a systematic review. Hum Exp Toxicol 2011;30:1119-40.
43. Isoda H, Talorete TP, Han J, Oka S, Abe Y, Inamori Y. Effects of organophosphorous pesticides used in China on various mammalian cells. Environ Sci 2005;12:9-19.
44. Krstić DZ, Colović M, Kralj MB, Franko M, Krinulović K, Trebse P, et al. Inhibition of AChE by malathion and some structurally similar compounds. J Enzyme Inhib Med Chem 2008;23:562-73.
45. Sanvicens N, Marco MP. Multifunctional nanoparticles–properties and prospects for their use in human medicine. Trends Biotechnol 2008;26:425-33.
46. Pan Y, Sabine Neuss, Annika Leifert, Monika Fischler, Fei Wen, Simon U, et al. Size-dependent cytotoxicity of gold nanoparticles. Small 2007;3:1941-9.
47. Momić T, Pašti TL, Bogdanović U, Vodnik V, Mraković A, Rakočević Z, et al. Adsorption of organophosphate pesticide dimethoate on gold nanospheres and nanorods. J Nanomater 2016;2016;1-11.
48. Nair AS, Pradeep T. Extraction of chlorpyrifos and malathion from water by metal nanoparticles. J Nanosci Nanotechnol 2007;7:1871-7.
49. Li H, Guo J, Ping H, Liu L, Zhang M, Guan F, et al. Visual detection of organophosphorus pesticides represented by mathamidophos using Au nanoparticles as colorimetric probe. Talanta 2011;87:93-9.
50. Yan X, Li H, Su X. Review of Optical Sensors for Pesticides. Trends Analyt Chem 2018;103:1-20.
51. Xia N, Wang Q, Liu L. Nanomaterials-based optical techniques for the detection of acetylcholinesterase and pesticides. Sensors (Basel) 2015;15:499-514.
52. Satnami ML, Korrama J, Nagwanshi R, Vaishanava SK, Karbhal I, Dewangan HK, et al., Gold nanoprobe for

inhibition and reactivation of acetylcholinesterase: An application to detection of organophosphorus pesticides. Sens Actuators B Chem 2018;267:155-64.

53. Chiang CW, Wang A, Mou CY. CO oxidation catalyzed by gold nanoparticles confined in mesoporous aluminosilicate Al-SBA-15: Pretreatment methods. Catal Today 2006;117:220-7.
54. Yakimovich NO, Ezhevskii AA, Guseinov DV,. Smirnova LA, Gracheva TA, Klychkov KS. Antioxidant properties of gold nanoparticles studied by ESR spectroscopy. Russ Chem Bull 2008;57:520-3.